2023 Theory & Simulation Performance Target: 3D MHD.

presentation given to Theory Coordinating Committee 10/30/23

1. The domestic & international, public & private stellarator community base their fusion reactor designs on 3D MHD equilibrium calculations.

   This TSPT sought to address the following:

Q1 Are our equilibrium codes (herein, VMEC, DESC & SPEC) accurate for the free-boundary calculation?

Yes; herein, we present quantitative comparisons, for relevant and challenging configurations.

Q2 Beyond the equilibrium, can we predict the nonlinear evolution of optimized stellarators?

Yes, using the extended-MHD code M3D-C1.

* Herein, only work performed under the TSPT will be presented. This is not a review.

** A lot of work was performed. For completeness, some of the following slides are detailed, but I will try to keep to the main topics.

Contributions from many individuals and institutions.

S. R. Hudson, A. M. Wright, C. Zhu, J. D. Hanson, A. Baillod, A. Giuliani, D. Panici, A. S. Ware, M. Cianciosa, J. Schmitt, M. Landreman, Z. Tecchiolli, F. Hindenlang, R. Köberl, R. Jorge, Z. Qu, E. J. Paul, L-M. Gerard, W. Sengupta, N. M. Ferraro, S. Saxena, J. Loizu, D. Dudt, & E. Kolemen.

Princeton Plasma Physics Lab. (PPPL)
U. Wisconsin–Madison
U. Science & Technology of China (USTC)
Auburn U.
École Polytechnique Fédérale de Lausanne (EPFL)
Flatiron Institute
Princeton U.
U. Montana
Oak Ridge National Lab. (ORNL)
Type One Energy Group
U. Maryland
Max-Planck-Institut für Plasmaphysik (IPP-Garching)
IST, U. Lisbon
Nanyang Technological University (NTU), Singapore
Columbia U.
U. Arizona

Outline.

1. Description of
    i. FOCUS, a Biot-Savart code;
    ii. VMEC, DESC and SPEC, inverse equilibrium codes; and
    iii. M3D-C1, an extended dynamical MHD code.
2. Two vacuum cases were studied, one with magnetic islands and one without (namely, the precise-QA case).
3. For each equilibrium calculation, we computed volume, surface and line integrals of the error.
4. Including pressure: VMEC and SPEC give the same Shafranov shift.
5. Allowing dynamics: extended MHD calculations performed using M3D-C1 for an optimized configuation.
6. Concluding comments.

7. Backup slides.

The FOCUS code for stellarator coil design gives "exact" vacuum magnetic field.

1. Given geometry, $\mathbf{x}_i(\theta)$, of a set of $i = 1, \ldots, N_C$ filamentary coils with current I_i, compute the magnetic field,

$$\mathbf{B}(\bar{\mathbf{x}}) = -\frac{\mu_0}{4\pi} \sum_{i=1}^{N_C} I_i \oint_i \frac{\mathbf{r} \times \mathbf{x}_i'}{r^3}\, d\theta, \text{ where } \mathbf{r} \equiv \bar{\mathbf{x}} - \mathbf{x}(\theta).$$

   i. Approximate coil by polygon; use Hanson & Hirshman [Phys. Plasmas **9**, 4410 (2002)] exact expression for $\mathbf{B}$.

2. Given geometry of *target surface*, $\mathcal{S}$, iteratively adjust the coil geometry to minimize

$$\mathcal{F}[\mathbf{x}_i] = \oint_{\mathcal{S}} \tfrac{1}{2} B_n^2\, ds + \omega \sum_{i=1}^{N_C} \oint_i dl, \text{ where } B_n \equiv \mathbf{B}(\bar{\mathbf{x}}) \cdot \mathbf{n},\ \omega \text{ is a } \textit{penalty}.$$

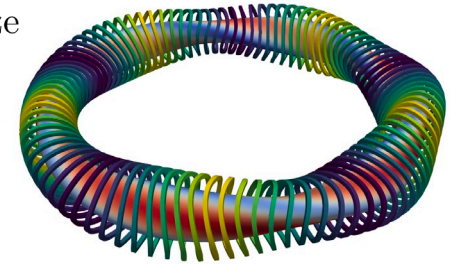

3. FOCUS [Zhu, Hudson *et al.*, Nucl. Fusion **58**, 016008 (2017)] used herein to

   i. construct coil sets for rotating elliptical boundary,

   ii. construct Poincaré plots, find magnetic axis, measure ι-profile,

   iii. construct input for free-boundary VMEC,
   $\mathbf{B} \cdot \hat{R}$, $\mathbf{B} \cdot \hat{\phi}$, $\mathbf{B} \cdot \hat{Z}$ on 3D *mgrid*, resolution N_R, N_ϕ, N_Z.

   iv. construct input for free-boundary SPEC,
   $(\sqrt{g}\mathbf{B} \cdot \mathbf{n})_{m,n}$ on "computational boundary", Fourier resolution M, N.

   v. FOCUS coil representation consistent with SIMSOPT coil representation.

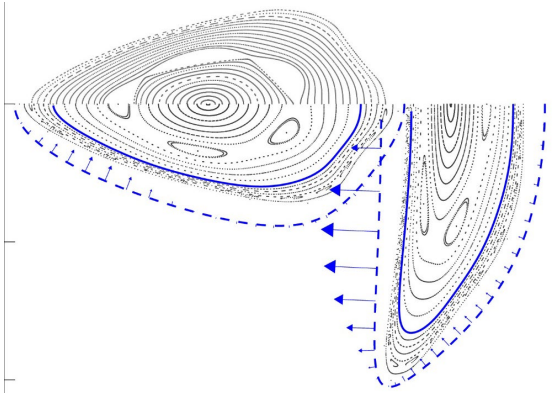

What is VMEC? Why is the vacuum calculation non-trivial?

1. VMEC remains the most widely used 3D ideal-MHD equilibrium code; used for design & reconstruction.
   i. Hirshman & Whitson, Phys. Fluids, **26**, 3553, (1983); Hirshman, van Rij & Merkel, Comp. Phys. Comm., **43**, 143 (1986).

2. The vacuum field is provided to free-boundary VMEC on input . . . so why is the vacuum calculation non-trivial?
   i. VMEC is an *inverse* equilibrium solver; assumes nested flux surfaces; pressure is a given function, $p = p(\psi)$.
   ii. The "degree-of-freedom" is geometry of nested flux surfaces, given by mapping $\mathbf{x}(\psi, \theta, \zeta) = x\,\mathbf{i} + y\,\mathbf{j} + z\,\mathbf{k}$.

3. Find minimum of energy functional, $\mathcal{W}[\mathbf{x}] \equiv \int_{\mathcal{V}} \left(\frac{p}{\gamma - 1} + \frac{B^2}{2\mu_0} \right) dv$, with respect to geometry of flux surfaces.
   i. For variation, $\boldsymbol{\xi} \equiv \delta\mathbf{x}$, and ideal constraint $\delta\mathbf{B} = \nabla \times (\boldsymbol{\xi} \times \mathbf{B})$, $\quad \delta\mathcal{W} = \int_{\mathcal{V}} \boldsymbol{\xi} \cdot (\nabla p - \mathbf{j} \times \mathbf{B})\, dv$.
   ii. For *free*-boundary calculations, the plasma boundary moves until $p(\psi_b) + \frac{1}{2}B^2\big|_{\partial\mathcal{V}^-} = \frac{1}{2}B^2\big|_{\partial\mathcal{V}^+}$

DESC is a "modern, improved" version of VMEC.

SPEC is based on multi-region relaxed MHD.

1. DESC:
   i. Assumes continously nested flux surfaces, inverse solver, based on ideal MHD (like VMEC).
   ii. Uses Fourier-Zernike polynomials (accurate near the magnetic axis).
   iii. Map to real-space collocation grid, compute $\mathbf{F} \equiv \nabla p - \mathbf{j} \times \mathbf{B}$, quasi-Newton method to minimize $\sum_{i,j,k} \mathbf{F}^2_{i,j,k}$.
   iv. Uses automatic differentiation (efficient calculation of gradients).
   v. Not just an equilibrium code, DESC is an integrated stellarator optimization package, c.f. SIMSOPT.
2. SPEC: stepped-pressure equilibrium code;
   i. Assumes a discrete set, $i = 1, \ldots, N_V$, of nested *interfaces*, between which the field is "Taylor relaxed".
   ii. Based on the multi-region relaxed MHD (MRxMHD) energy functional; inverse solver;

$$\mathcal{F} \equiv \sum_{i=1}^{N_V} \left[\int_{\mathcal{V}_i} \left(\frac{p_i}{\gamma - 1} + \frac{B_i^2}{2\mu_0} \right) dv + \frac{\mu_i}{2} \left(\int_{\mathcal{V}_i} \mathbf{A}_i \cdot \mathbf{B}_i \, dv - H_i \right) \right].$$

   iii. In each region, $p_i = const.$ and $\nabla \times \mathbf{B}_i = \mu_i \mathbf{B}_i$; on the interfaces, $\mathbf{B} \cdot \mathbf{n} = 0$; and across, $[[p + B^2/2]] = 0$.

M3D-C1 is an extended-MHD initial-value code (can perform dynamical simulations).

1. We use the single-fluid model in M3D-C1, as described by the equations below.
   i. Similiar capability (NIMSTELL) under construction with NIMROD.
2. Compared to the equilibrium calculation, this is a higher fidelity model.
   i. No constraints on the magnetic field topology (no sheet currents, allows for magnetic islands and irregular fieldlines).
   ii. No constraints on the pressure: anisotropic thermal transport (so that the pressure "evolves" self-consistently with **B**).
   iii. With isotropic viscosity, with and realistic transport/dissipation parameters.

$$\frac{\partial n_i}{\partial t} + \nabla \cdot (n_i \mathbf{v}) = \nabla \cdot (D \nabla n_i), \tag{1}$$

$$m_i n_i \left(\frac{\partial \mathbf{v}}{\partial t} + \mathbf{v} \cdot \nabla \mathbf{v} \right) = \mathbf{j} \times \mathbf{B} - \nabla p - \nabla \cdot \mathbf{\Pi}, \tag{2}$$

$$n_e \left[\frac{\partial T_e}{\partial t} + \mathbf{v} \cdot \nabla T_e + (\gamma - 1) T_e \nabla \cdot \mathbf{v} \right] = (\gamma - 1) \left[\eta j^2 - \nabla \cdot \mathbf{q}_e \right], \tag{3}$$

$$n_i \left[\frac{\partial T_i}{\partial t} + \mathbf{v} \cdot \nabla T_i + (\gamma - 1) T_i \nabla \cdot \mathbf{v} \right] = (\gamma - 1) \left[-\mathbf{\Pi}_i : \nabla \mathbf{v} - \nabla \cdot \mathbf{q}_i \right], \tag{4}$$

$$\mathbf{E} = \eta \mathbf{j} - \mathbf{v} \times \mathbf{B}, \tag{5}$$

where $\mathbf{j} = \nabla \times \mathbf{B}/\mu_0$, $\gamma = 5/3$, and $\mathbf{q}_s = -\kappa_s \nabla T_s - \kappa_{s,\parallel} \mathbf{b}\,\mathbf{b} \cdot \nabla T_s$, and $\mathbf{\Pi}_i$ is an isotropic viscosity.

Comparisons performed for vacuum fields with and without magnetic islands.

1. For the precise-QA case, which does not have islands, and for a vacuum field with islands (not optimized), error measures were calculated. (to be described next slide).

2. Using FOCUS, free-boundary VMEC, free-boundary SPEC, and fixed-boundary DESC.

	Poincaré plot FOCUS/VMEC/SPEC	ι profile FOCUS/VMEC/SPEC	Poincaré plot FOCUS/DESC	ι-profile FOCUS/VMEC/DESC
precise-QA	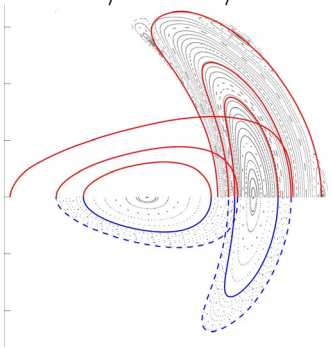	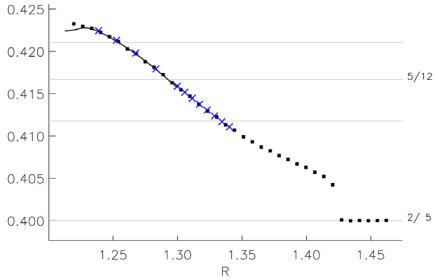	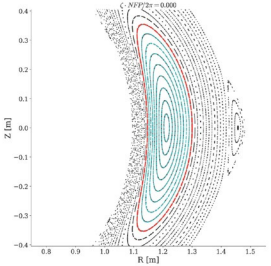	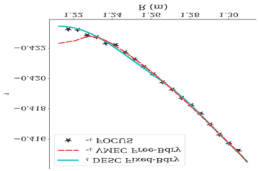
islands	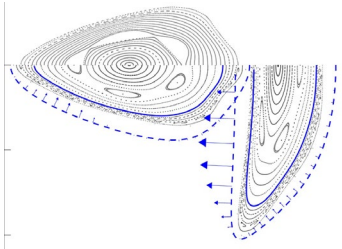	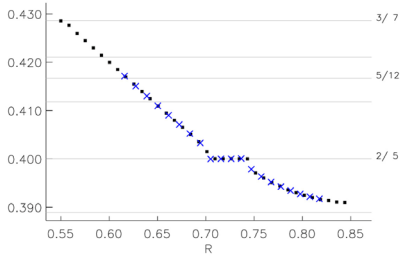	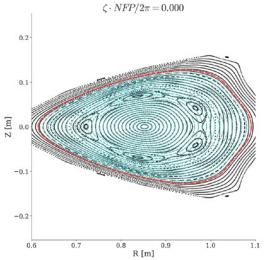	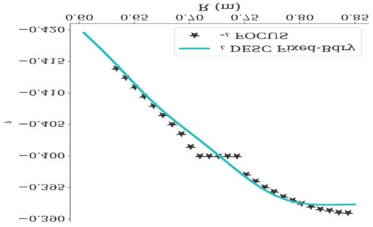

To make quantitative comparisons, we calculated volume, surface and line integrals of dimensionless errors.

1. Given a numerical approximation, $\mathbf{B}_h$, to the exact magnetic field, $\mathbf{B}$, introduce:

   i. Error in total energy, $\delta E \equiv \frac{1}{E}(E_h - E)$, where $E \equiv \int_{\mathcal{V}} \frac{1}{\mu_0} B^2 \, dv$.

   ii. Volume-integrated relative pointwise error, $||\delta B|| \equiv \frac{1}{V} \int_{\mathcal{V}} \frac{|\delta \mathbf{B}|}{|\mathbf{B}|} \, dv$, where V is plasma volume.

   iii. Error in normal field on boundary, $\delta b_n \equiv \frac{1}{S} \int_{\mathcal{S}} \frac{|\mathbf{B} \cdot \mathbf{n}|}{|\mathbf{B}|} \, ds$, where $\mathcal{S} = \partial \mathcal{V}$, $S \equiv \int_{\mathcal{S}} ds$, with unit normal, $\mathbf{n}$.

   iv. Error in geometry of magnetic axis, $E_A \equiv \frac{1}{L} \int_{\mathbf{x}} \frac{|\delta \mathbf{x}|}{|\mathbf{x}|} \, dl$, where $\mathbf{x}(\phi)$ is the magnetic axis, $L \equiv \int_{\mathbf{x}} dl$.

2. For vacuum fields, the "exact" magnetic field is provided by FOCUS.

For the precise-QA and the vacuum field with islands, the errors were computed.*

		Φ_{edge} (W)	V (m^3)	δb_n	δE	$\|\|\delta B\|\|$
precise QA	VMEC	0.025	0.558	3.4×10^{-5}	3.9×10^{-6}	1.3×10^{-4}
precise QA	VMEC	0.050	1.130	7.1×10^{-5}	7.4×10^{-6}	1.6×10^{-4}
precise QA	VMEC	0.120	2.840	3.9×10^{-3}	2.5×10^{-3}	3.9×10^{-3}
precise QA	SPEC	0.025		5.3×10^{-6}	3.6×10^{-11}	7.5×10^{-6}
precise QA	DESC*	0.030	0.676	5.3×10^{-6}	3.9×10^{-6}	9.7×10^{-5}
island case	VMEC*		0.597	7.9×10^{-5}	8.6×10^{-5}	3.1×10^{-4}
island case	SPEC	0.012	0.246	1.5×10^{-4}	5.4×10^{-9}	2.8×10^{-4}
island case	DESC*		0.599	1.5×10^{-4}	8.1×10^{-6}	2.8×10^{-4}

* The above data is as presented in the Second Quarter Report, submitted in March, 2023. The errors are all small, higher resolution calculations may lower the errors further, and code-development work ongoing for each code.

1. Impressive that the 3 leading 3D MHD equilibrium codes:
   i. compute the same error measures, and all the errors are small,
   ii. for 2 very relevant and challenging vacuum fields,
   iii. without *a priori* knowledge of the results. Great scientific cooperation.
2. These configurations are now standard test cases for 3D MHD codes.

Beyond the vacuum: including pressure in 3D, free-boundary equilibria.

1. VMEC is based on ideal MHD; SPEC is based on multi-region relaxed MHD; should agree when $N_V \to \infty$.
   i. But what about when $N_V = 8$? Must choose stepped pressure $p_i(\psi_{i+1} - \psi_i) = \int_{\psi_i}^{\psi_{i+1}} p(\psi)\, d\psi$.

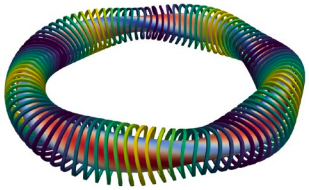

2. Calculation performed in rotating elliptical geometry, $p(\psi) = p_0(1 - \psi)$, $I(\psi) = 0$.

Poincaré plot
FOCUS/VMEC/SPEC

ι profile
FOCUS/VMEC/SPEC

p profile

magnetic axis
FOCUS/VMEC/SPEC

vacuum

"high-β"

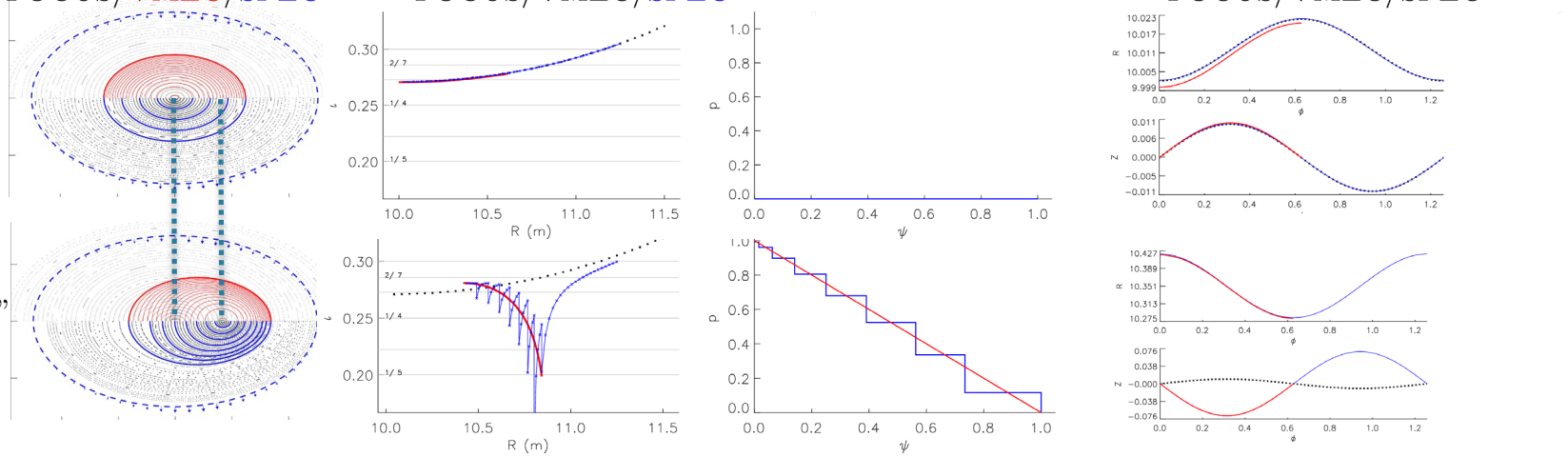

3. "Lowest-order integral property" is the Shafranov shift.
   i. Despite evidence of a small error in VMEC near the magnetic axis, VMEC and SPEC agree on the shift of the magnetic axis.
   ii. See back-up slide for discontinuities in SPEC ι.

error in magnetic axis	E_{FV}	E_{FS}	E_{SV}
vacuum	1.4×10^{-4}	1.1×10^{-5}	1.4×10^{-4}
high-β	n/a	n/a	1.3×10^{-4}

For an optimized stellarator, the nonlinear evolution was simulated using M3D-C1

1. For an equilibrium that was optimized for self-consistent bootstrap current, quasi-symmetry and good energetic-particle confinement [Landreman *et al.*, Phys. Plasmas, **29**, 082501 (2022)].

2. The equilibrium is MHD unstable. Flux surfaces near the edge breakup and form an *ergodic sea*.

   i. (top row): Poincaré plots at $t = 0\ \tau_a$ (left) and at $t = 825\ \tau_a$ with constant (middle) and Spitzer (right) resistivity profiles.

   ii. (bottom row): Electron temperature profiles on the $\phi = 90^o$ cross-section.

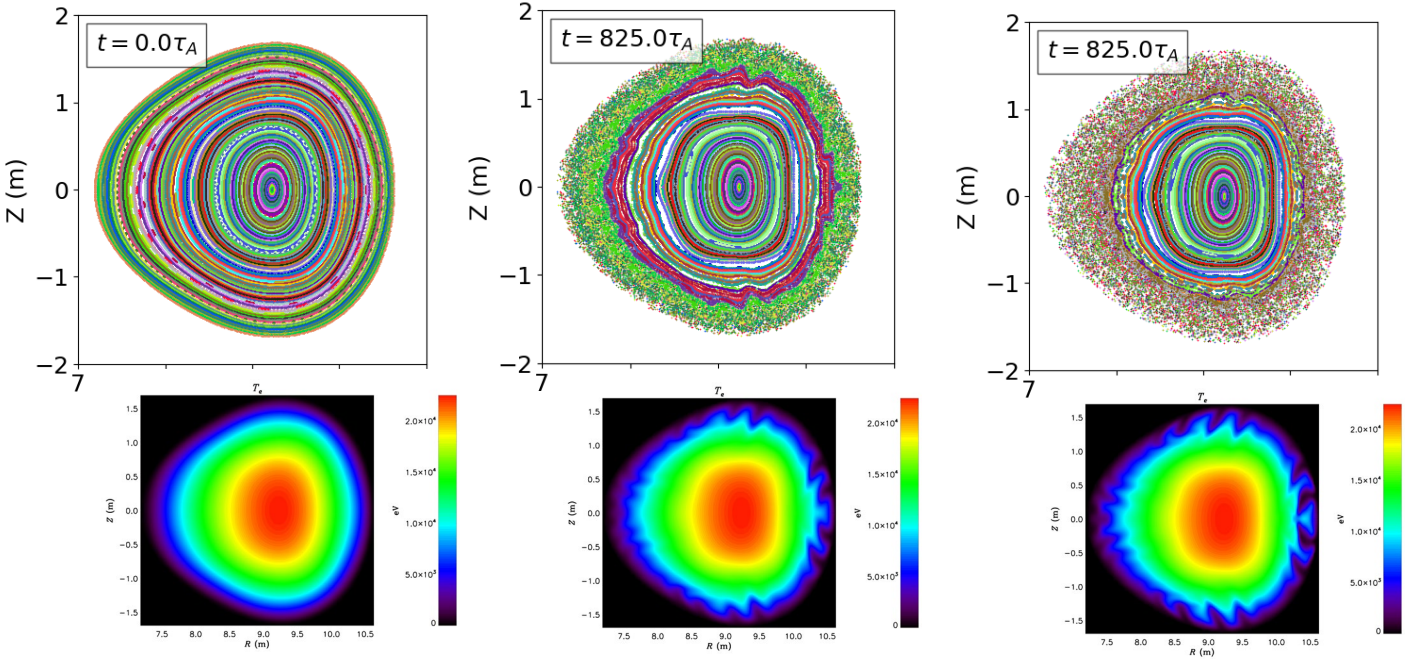

2023 Theory & Simulation Performance Target: 3D MHD: Summary.

1. The US stellarator community is very competent in the 3D MHD equilibrium calculation.
   i. VMEC, SPEC and DESC are the world's leading equilibrium codes.
   ii. We are pursuing complementary approaches and comparing quantitative measures of the error.

2. Following recent development of M3D-C1, we have unique capability in the simulation of stellarator dynamics.
   i. Similiar capability is expected from NIMSTELL.

3. The US has a dominant leadership position in the macroscopic modeling of stellarators.
   i. This is all because of sustained DOE investment.

4. Backup slides: i. Quarterly Milestones. ii. Convergence of free-boundary VMEC for precise-QA case. iii. Convergence of rotational-transform, ι_a, computed by VMEC near the magnetic axis. iv. *Extremely* shaped configurations that pose challenges, and our solutions. v. Single "sharp-boundary" configuration: a discontinuity in pressure, $p(\psi)$, can induce a discontinuity in $\iota(\psi)$. vi. Analysis of instability growth rates for an optimized stellarator using M3D-C1. vii. Some relevant papers that describe DESC and its application to stellarator design. viii. Some relevant papers that describe SPEC and its application to understanding 3D magnetohydrostatic equilibria.

Theory & Simulation Performance Target: Quarterly Milestones:

1. Milestones were ambitious, and were completed.

   Calculating the magnetohydrodynamic (MHD) equilibrium state in strongly shaped stellarators, including W7-X and other designs, is essential for understanding stellarator performance. The free-boundary calculation, in which the location of the plasma boundary is determined self-consistently given the externally applied magnetic field, is particularly important because of the need to understand the transport of heat and particles across the edge of the plasma, which is generally partially chaotic.

   We shall complete a hierarchy of verification calculations of 3D MHD equilibrium codes, in particular the widely used VMEC code, which assumes nested flux surfaces, and the SPEC code, which does not and which also accommodates the formation of singular currents. We shall explore cases for which these codes should agree, and cases for when they should not. We shall prepare the necessary code interfaces so that equilibrium information can be used to initialize initial value codes, such as M3D-C1, so that the nonlinear stability of 3D equilibria can be investigated.

1. 1st Quarter

   In a relevant, non-axisymmetric geometry with a supplied set of external currents, perform a free-boundary verification calculation between VMEC and SPEC. The first calculation should consider the vacuum case, for which the equilibrium magnetic field of both codes can be compared to the magnetic given calculated using the Biot-Savart law.

2. 2nd Quarter

   Perform an investigation of the consequences of introducing a magnetic island into the vacuum equilibrium field, both inside and outside the VMEC/SPEC computational boundary, and explore how this affects the comparison between the codes and the vacuum field.

3. 3rd Quarter

   Repeat the verification calculations with increasing pressure profiles, and with either the helicity, current or rotational-transform profiles included as constraints.

4. 4th Quarter

   Explore configurations of interest – both existing stellarators and current designs – with increasing realistic plasma profiles. Initialize the M3D-C1 extended-MHD initial-value code with a relevant equilibrium to explore code performance, and explore transport of pressure, for example.

Verification calculation for free-boundary VMEC for the precise-QA vacuum.

1. For Landreman & Paul's *precise-QA* configuration, with coils constructed Wechsung *et al.*.
2. A high-resolution mgrid file was constructed, with $N_R = 512$, $N_Z = 512$, and $N_\phi = 720$.
3. A series of free-boundary, zero-pressure, zero-current VMEC calculations was performed.
4. The error, $E_V \equiv \int_{\mathcal{V}} \delta\mathbf{B} \cdot \delta\mathbf{B}\, dv$, where $\delta\mathbf{B} \equiv \mathbf{B}_V - \mathbf{B}_F$, is shown to reliably decrease.
5. A fixed-boundary SPEC calculation, using the boundary computed by free-boundary VMEC, was performed, also with low error.

precise-QA & coils

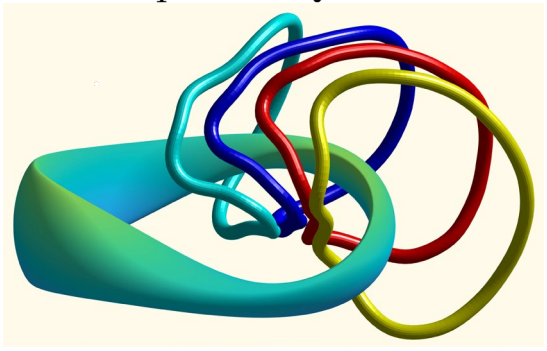

Poincaré plot

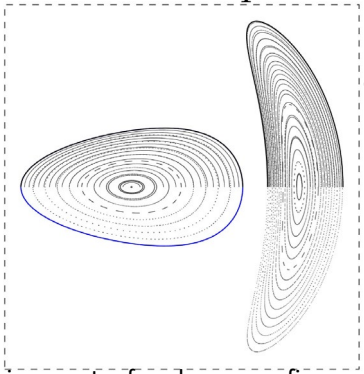

ι-profile

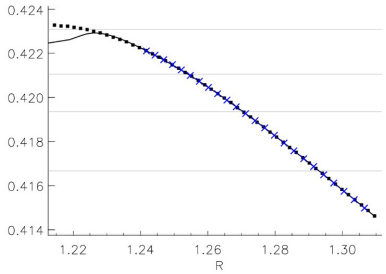

convergence

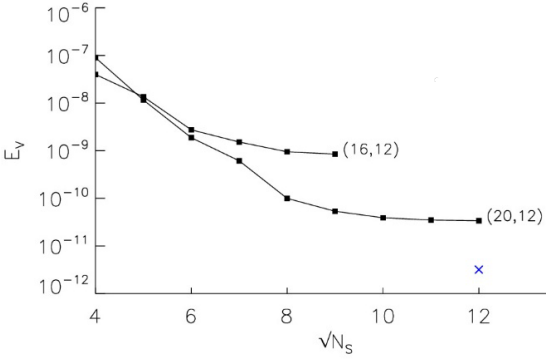

Landreman & Paul, "Magnetic fields with precise quasisymmetry for plasma confinement", Phys. Rev. Lett., 128:035001 (2022)
Wechsung, Landreman *et al.*, "Precise stellarator quasi-symmetry can be achieved with electromagnetic coils", Proc. Nat. Acad. Sci., 119(13):2202084119 (2022)

Investigating the near-axis resolution issue in VMEC.

1. Near the magnetic axis, VMEC converges slower than expected; error $\propto \Delta s^1$ instead of error $\propto \Delta s^2$.

   i. induces a "spurious current" near the axis, which complicates equilibrium reconstruction.

   ii occurs for axisymmetric equilibria; e.g. analytic Grad-Shafranov equilibrium with constant ι,

3. Current amelioration efforts focussed on finite differencing near the axis.

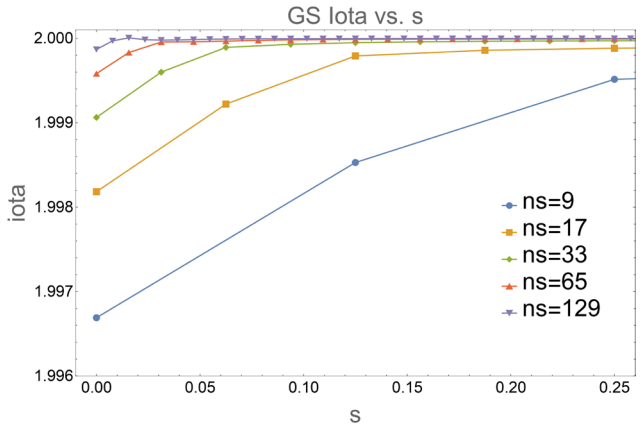

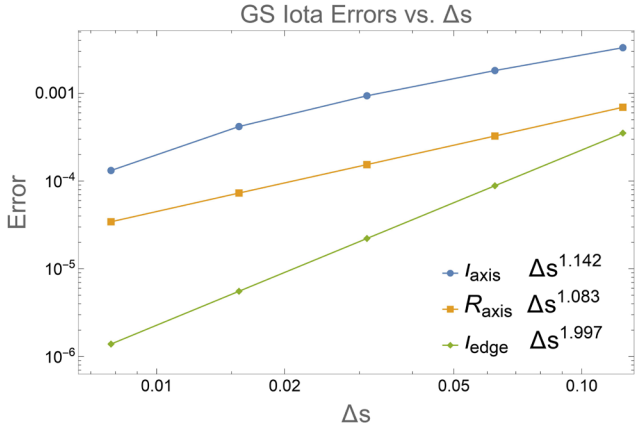

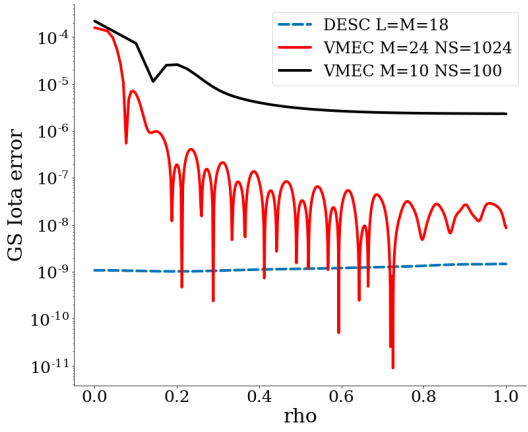

Extremely shaped configurations from near-axis expansions can cause difficulties; but, the difficulties we can overcome using 2 different methods.

1. The avant-garde configurations optimized using near-axis expansions are so strongly shaped that existing algorithms for constructing nested coordinate surfaces can fa

2. E.g., a 2-field-period, quasi-helical case from Landreman [J. Plasma Phys., **88**, 905880616 (2022)].

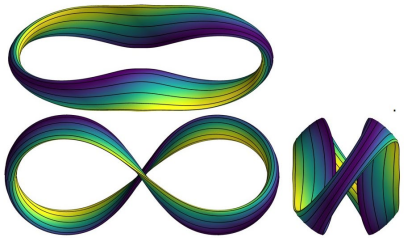

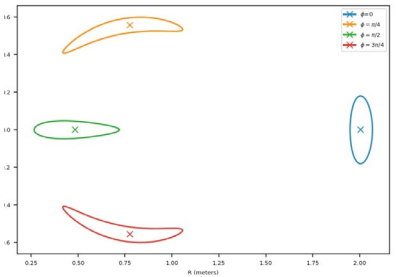

3. Solution Method One: slowly increase shaping, implemented in DESC (see lower right). [Conlin *et al.*, J. Plasma Phys. **89**, 955890305 (2023)]

4. Solution Method Two: "Robust" coordinates: (see below)

   choose mapping, $\mathbf{x}(s,\theta,\zeta)$, that minimizes $\mathcal{F}_c = \int_0^1 ds \int_0^{2\pi} d\theta \int_0^{2\pi} d\zeta \left[\frac{\sqrt{g}}{s}\sqrt{g} + \omega\sqrt{\mathbf{x}_s \cdot \mathbf{x}_s} \right.$

   i. New method tested [Tecchiolli, Hudson & Loizu, in preparation] and implemented in GVEC.

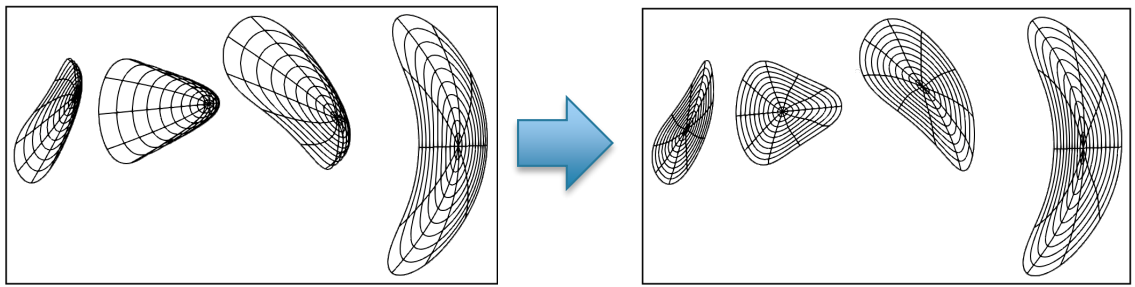

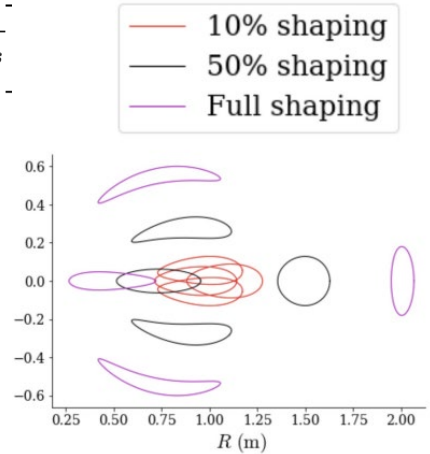

To compare VMEC & SPEC, consider a "sharp-boundary" equilibrium.

1. Instead of a stepped approximation to a continuous profile, consider a polynomial approximation to a stepped profile.

Poincaré plot

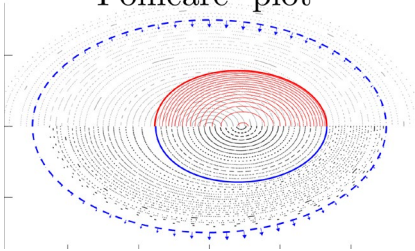

ι-profile

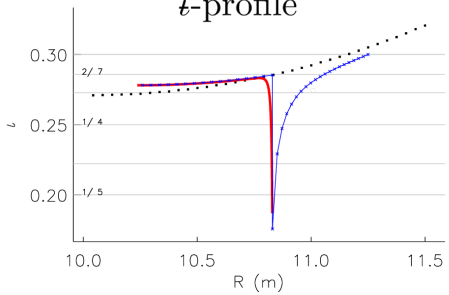

$p(\psi) = p_0(1 - \psi^{16})$

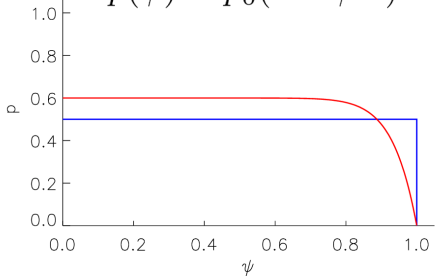

2. Placing all of the pressure gradient on/near the edge drives a localized pressure-driven current, which creates a local discontinuity in ι.

3. For *verification*: the point is, when given the same pressure profile, that free-boundary VMEC and free-boundary SPEC agree.

4. For *validation*: well, validation is beyond this TSPT.

   i. Theoretically, MRxMHD can have arbitrarily many steps, e.g. Hudson, Dewar *et al.*, Phys. Plasmas, **19**, 112502 (2012).

   ii. Numerical implementation: the nonlinear solver and spectral representation in SPEC is clumsy; SPEC is fragile for large N_V in strongly shaped geometries.

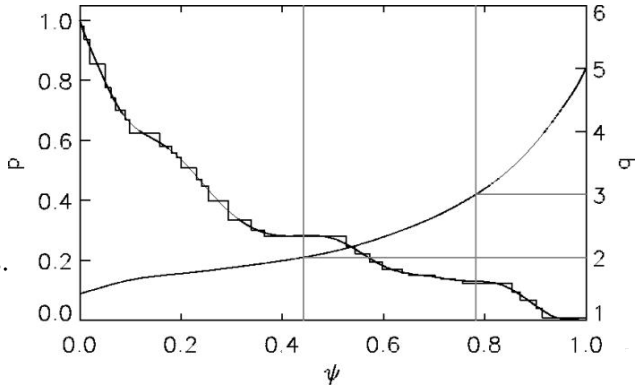

Using M3D-C1, can perform eigenmode analyses, measure growth rates, . .

1. (Right) Growth rates of the kinetic energy for various n's for uniform (dashed) and Spitzer (solid) resistivity profiles.

2. (Below) Toroidal Fourier components of the magnetic energy, as a function of time (for Spitzer) resistivity,

   i. stellarator-mode coupling: for this $N_{FP} = 2$, a single unstable eigenmode will include all even-n toroidal Fourier modes.

3. In future work, incorporate self-consistent bootstrap current, can provide additional poloidal field & transform in quasi-symmetric stellarators, adding 2-fluid or kinetic effects.

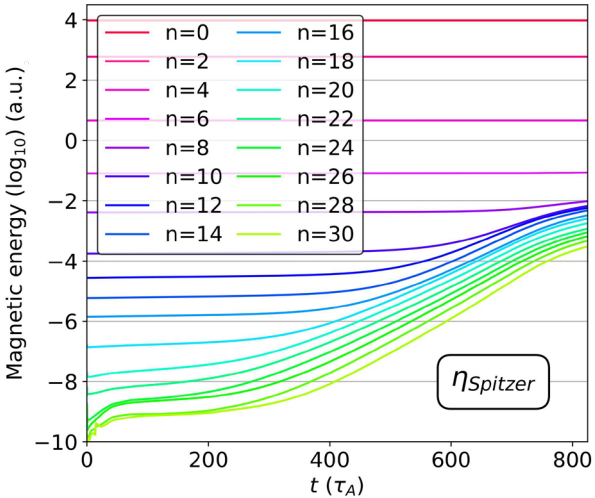

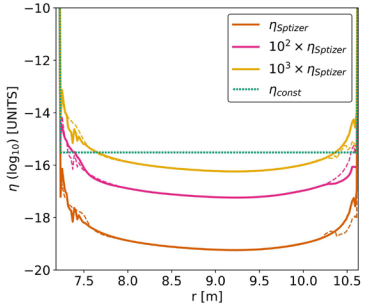

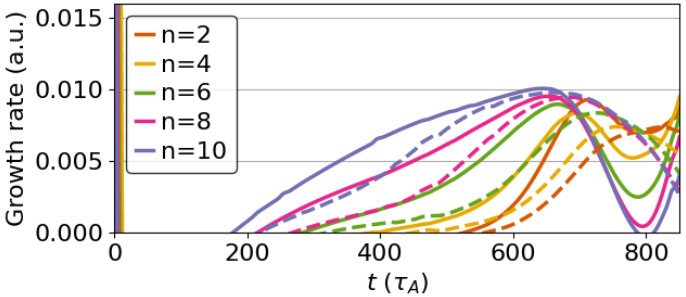

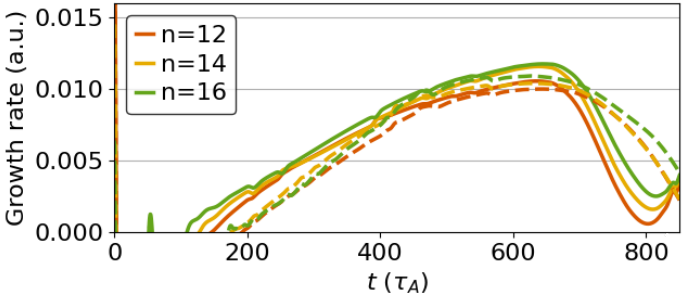

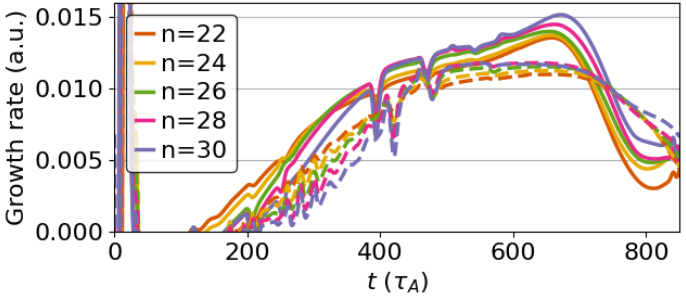

1. DESC code developed and verified against VMEC [D. W. Dudt and E. Kolemen, DESC : A stellarator equilibrium solver, Phys. Plasmas 27, 102513 (2020)]

2. DESC code shown to accurately resolve equilibria, especially at axis, better than VMEC and comparing well to near-axis expansion theory [D. Panici, R. Conlin, D. W. Dudt, and E. Kolemen, The DESC stellarator code suite part 1: Quick and accurate equilibria computations, J. Plasma. Phys. (2023)]

3. DESC perturbation methods developed and shown to robustly and efficiently find highly shaped and high-beta equilibria [R. Conlin, D. W. Dudt, D. Panici, and E. Kolemen, The DESC stellarator code suite part 2: Perturbation and continuation methods, J. Plasma. Phys. (2023).]

4. DESC code shown to perform stellarator optimization orders of magnitude faster than previous methods such as STELLOPT, owing to its automatic differentiation, perturbation methods, and GPU capabilities [D. W. Dudt, R. Conlin, D. Panici, and E. Kolemen, The DESC stellarator code suite part 3: Quasi-symmetry optimization, J. Plasma. Phys. 89, 955890201 (2023).]

5. Capability to optimize for general omnigenity developed in DESC and used to optimize in previously unexplored phase space regions [D. W. Dudt, R. Conlin, D. Panici, A. G. Goodman, and E. Kolemen, Magnetic Fields with General Omnigenity, PNAS, submitted.]

The stepped-pressure equilibrium code computes multi-region relaxed MHD

1. Bruno & Laurence [Commun. Pure App. Math. **49**, 717 (1996)] proved the existence of stepped-pressure equilibria when the nonaxisymmetry is small, with the interfaces having sufficiently irrational ι, and with an arbitrary number of pressure jumps; building on original work by Berk *et al.* [Phys. Fluids **29**, 3281 (1986)].

2. Hudson, Dewar, Hole *et al.* [Phys. Plasmas **19**, 112502 (2012)] developed SPEC, which finds stationary points of the MRxMHD energy functional, $\mathcal{F} \equiv \sum_{i=1}^{N_V} \left\{ \int_{\mathcal{V}_i} \left[\frac{p}{\gamma - 1} + \frac{B^2}{2} \right] dv + \nu \left[\int_{\mathcal{V}_i} \mathbf{A} \cdot \mathbf{B}\, dv - H_i \right] \right\}$.

3. Free-boundary capability [Hudson, Loizu, Zhu *et al.*, Plasma Phys. Contr. Fusion, **62**, 084002 (2020)].

4. Enciso *et al.* [J. European Math. Soc., to appear] proved that the toroidal domains do not need to be small perturbations of an axisymmetric domain.

5. Huang *et al.* [Phys. Plasmas **23**, 032513 (2022)] computed the singular currents in ideal MHD equilibria using SPEC by taking $N_V \to \infty$.

6. Not just an equilibrium code, also a linear stability code. Kumar *et al.* [Plasma Phys. Control. Fusion **65**, 075004 (2023)] demonstrated that SPEC recovers linear-ideal and -resistive stability.

7. Loizu & Bonfiglio [J. Plasma Phys., **89**, 905890507 (2023)] show that saturation of tearing modes can be calculated with SPEC; Wright *et al.* [J. Plasma. Phys., (2022)] show comparisons of SPEC and M3D-C1.

8. SPEC used to understand self-organization/double-axis states in RFPs [Phys. Rev. Lett., **111**, 055003 (2013), Phys. Lett. A, **462**, 128664 (2023)]. Aleynikova *et al.* [Nucl. Fusion, **61**, 126040 (2021)] used SPEC for interpretation of current-drive-induced crash cycles in W7-X as partial/global relaxation events.

9. SPEC used in SIMSOPT optimization for nested surfaces at nonzero β [Baillod *et al.*, Phys. Plasmas **29**, 042505 (2022)].